ISSN 1063-7788, Physics of Atomic Nuclei, 2021, Vol. 84, No. 10, pp. 1734–1742. © Pleiades Publishing, Ltd., 2021.

ENGINEERING DESIGN OF EQUIPMENT FOR NUCLEAR PHYSICS

Magneto-Optical Structure of the NICA Collider with High Transition Energy

S. D. Kolokolchikov[a,b,*] and Y. V. Senichev[a,b]

[a] *Institute for Nuclear Research of Russian Academy of Sciences, Moscow, 117312 Russia*

[b] *Moscow Institute of Physics and Technology, Dolgoprudny, Moscow oblast, 141701 Russia*

**e-mail: sergey.bell13@gmail.com*

Received July 19, 2021; revised August 9, 2021; accepted August 9, 2021

Abstract—Methods of increasing the transition energy for the proton option of the NICA collider are investigated. The method of superperiodic modulation of quadrupole gradients is applied. The selection of sextupoles is carried out to suppress the natural chromaticity and compensate for the sextupole component. The Twiss parameters for the proposed structures are given, as well as the dynamic apertures and working points are investigated.

Keywords: transition energy, superperiod, dispersion suppression, chromaticity suppression

DOI: 10.1134/S1063778821100185

1. PROTON MODE OF NICA COLLIDER.

First of all the structure of the NICA collider was designed to work in two modes: for experiments with heavy ions $^{79}Au_{197}$ and for experiments with polarized protons/deuterons p, d. At the maximum collision energy in the heavy ion collision experiment of 4.5 GeV/nucleon, the transition energy of the magneto-optical structure of the collider is $E_{tr}^{Au-Au} = 5.7$ GeV ($\gamma_{tr}^{Au-Au} = 7.1$). In this case, there are no problems with the transition through the transition energy that was originally taken into account when designing. This value of the transition energy was achieved by choosing the frequency of betatron oscillations in the horizontal plane $\nu_x \approx \gamma_{tr}^{Au} > \gamma_{max}^{Au} \approx 7.1$, which is subject to the regularity of the structure of the arcs consisting of identical cells of the FODO, must be greater than the maximum value of the Lorentz factor in the entire energy range. This regularity condition of the structure is simultaneously necessary to minimize the modulation of the beam envelope, coinciding with the condition of minimizing the effect of intrabeam scattering in the heavy-ion option with a large particle charge. Small perturbations at the edges of the arc due to the dispersion suppressors by the missing magnet method do not play a fundamental role in all of the above.

Crossing through the transition energy, a longitudinal instability develops. Threshold current of its instability development $I_{th} \sim \eta$ proportional to the slip-factor η, which is equal to zero when $\gamma = \gamma_{tr} = 7.1$. At transition, the rate of acceleration of protons using the induction acceleration of the RF1 station is $d\gamma/dt = 0.2$ s^{-1}. This rate is too small to avoid the development of instability when the relativistic factor approaches to γ_{tr}.

The magnetic rigidity of the rotary magnets is constant $R_{arc}B_{bend} = \dfrac{Amc\gamma\beta}{eZ} \approx 45$. Thus, the maximum possible energy in the proton acceleration experiment is determined $E_{max}^{p} = 12.4$ GeV ($\gamma^{p} = 14.3$), therefore, the gamma-transition must be at the level of $\gamma_{tr}^{p} \sim 15$–16, which is obviously higher than the transition energy for an ionic regular structure $E_{tr}^{Au-Au} = 5.7$ GeV ($\gamma_{tr}^{Au-Au} = 7.1$). In order to exclude the crossing through the transition energy during proton acceleration, a new optical ring structure must be implemented for the proton mode instead of the optical structure of the ion mode. In this optical structure, the transition energy must be higher than the maximum proton energy when the collider is operating for the experiment.

For a proton beam with an intensity of 2×10^{13} the time of intrabeam heating increases by about 30 times compared to beams of gold ions with an intensity of 6.6×10^{10}. Therefore, the transition energy can rise due to the variation of the dispersion without fear of the influence of intrabeam scattering. Due to the resonant modulation of the dispersion function, the diffusion coefficient for intrabeam scattering increases by 2–3 times, this is not critical both when protons are

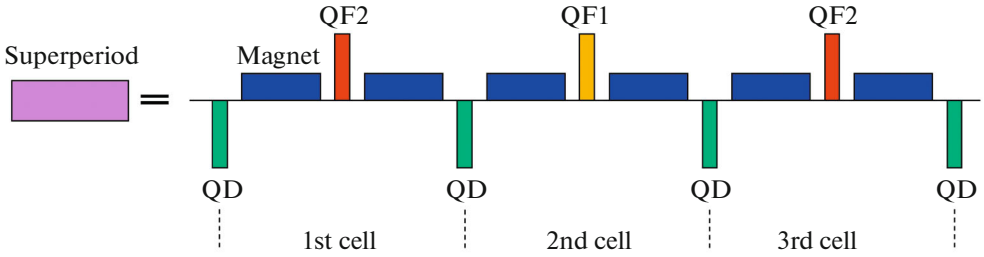

Fig. 1. Introduction of a superperiod consisting of 3 FODO cells.

cooled during accumulation, and when they are grouped at the energy of the experiment.

2. SUPERPERIODIC MODULATION

The momentum compaction factor is defined in [1] as

$$\alpha = \frac{1}{\gamma} = \frac{1}{C}\int_0^C \frac{D(s)}{\rho(s)}ds, \qquad (1)$$

where C is the the length of a closed equilibrium orbit, $D(s)$ is the horizontal dispersion function, $\rho(s)$ is the radius of curvature of the equilibrium orbit.

Equation for the dispersion function with biperiodic variable focus

$$\frac{d^2D}{ds^2} + \left[K(s) + \varepsilon k(s)\right]D = \frac{1}{\rho(s)}, \qquad (2)$$

where $K(s) = \frac{e}{p}G(s)$, $\varepsilon k(s) = \frac{e}{p}\Delta G(s)$, $G(s)$ is the gradient of magneto-optical lenses, $\Delta G(s)$ is the superperiodic gradient modulation. A superperiod is defined as a combination of several FODO cells as shown in Fig. 1. Thus, in the general case, the coefficient of expansion of the orbit depends on the functions: the curvature of the orbit $\rho(s)$, gradient and modulation of quadrupole lenses respectively $G(s)$, $\Delta G(s)$. In the NICA structure, the regular arrangement of dipole magnets eliminates the possibility of modulating the curvature of the orbit. Therefore, we use only the modulation of the strength of the quadrupole lenses over the length of the superperiod. Function $K(s)$ has a periodicity of one period of the focusing cell, $k(s)$ has a superperiod periodicity. For one superperiod, the momentum compaction factor is determined by the formula (3), the conclusion of this formula is made in [1]:

$$\alpha_s = \frac{1}{\nu_{x,\mathrm{arc}}^2}\left\{1 + \frac{1}{4}\left(\frac{\bar{R}_{\mathrm{arc}}}{\nu_{x,\mathrm{arc}}}\right)^4 \times \sum_{k=-\infty}^{\infty}\frac{g_k^2}{(1 - kS/\nu_{x,\mathrm{arc}})[1 - (1 - kS/\nu_{x,\mathrm{arc}})^2]^2}\cdots\right\}, \qquad (3)$$

where $\bar{R}_{\mathrm{arc}}$ is the the average value of the curvature, $\nu_{x,\mathrm{arc}}$ is the the number of horizontal betatron oscillations on the length of the arc, S is the number of superperiods per arc length, g_k is the kth harmonic of the gradient modulation in the Fourier series expansion of the function $\varepsilon k(s) = \sum_{k=0}^{\infty} g_k \cos(k\phi)$. Due to the mirror symmetry, the decomposition is performed in cosines. In the absence of superperiodic modulation $g_k = 0$, $\forall k$, formula (3) takes the form $\alpha_s = \frac{1}{\nu_{x,\mathrm{arc}}^2}$, which corresponds to the case of a regular structure. To raise the transition energy, it is necessary to reduce $\alpha_s = 1/\gamma_{\mathrm{cr}}^{\mathrm{arc}}$, this means that the expression under the sum sign must be negative, this is realizable under the condition $\frac{kS}{\nu_{x,\mathrm{arc}}} > 1$. First harmonic $k = 1$ has a dominant influence and for 12 FODO cells, the condition is implemented $S = 4$, $\nu_{x,\mathrm{arc}} = 3$, where 3 FODO cells are combined into one superperiod. Thus, due to the tune of betatron oscillations of a multiple of 2π, the arc has the properties of a first-order achromate.

Previously, all formulas were given for the arc, and not for the entire ring of the collider. The insertion of straight sections reduces the degree of modulation of the dispersion function. The average value of the dispersion decreases with a longer orbit length, this means that the momentum compaction factor decreases for the entire accelerator, and the resulting value of the gamma-transition $\gamma_{\mathrm{tr}}^{\mathrm{total}}$ increases and is determined in [2] by the expression:

$$\gamma_{\mathrm{tr}}^{\mathrm{total}} = \gamma_{\mathrm{tr}}^{\mathrm{arc}}\sqrt{\frac{SL_s + L_{\mathrm{str}}}{SL_s}}. \qquad (5)$$

Table 1. Values of arc quadrupole gradients in case of dispersion suppression by edge cells

Quadrupoles	Gradient, T/m
QF1	28.26481
QF2	20.9276
QD	22.62231
QFE1	30.9342
QFE2	19.58429

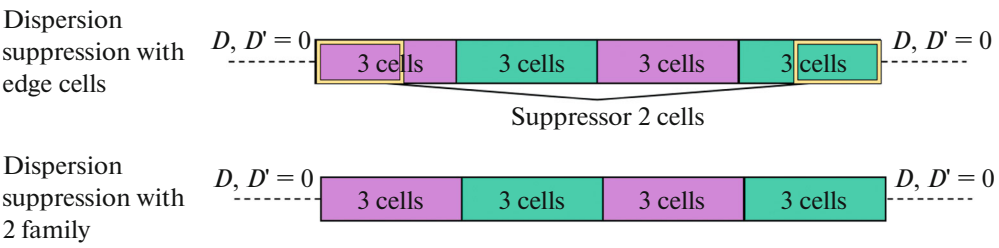

Fig. 2. Schematic diagram of two possible dispersion suppression options for the proton option of the NICA collider.

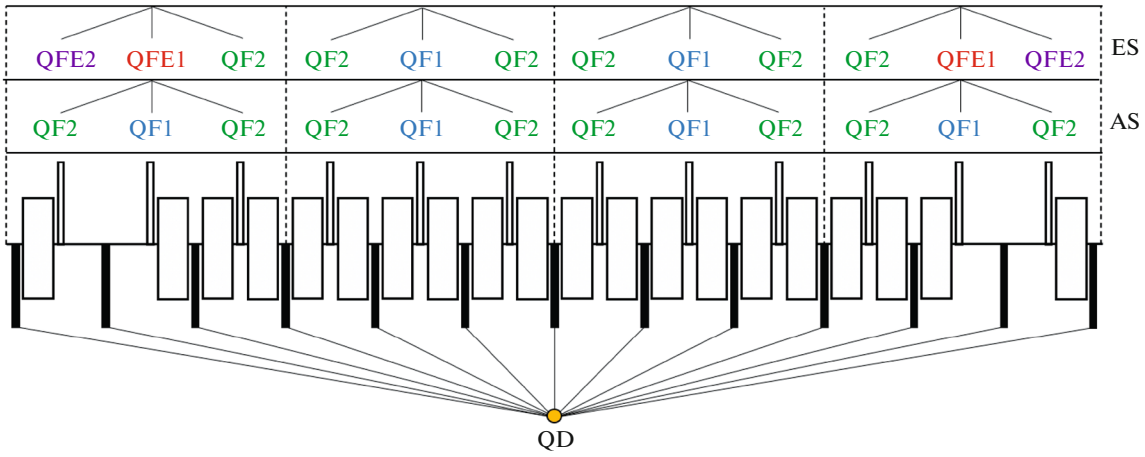

Fig. 3. The scheme of arrangement of quadrupoles on the arc of the accelerating ring, providing a variation of the transition energy and performing the function of dispersion suppression in straight sections. The case with the possibility of dispersion suppression by edge superperiods (Edge suppressor) is shown above. Below, the dispersion is suppressed only by matching the gradients of two families of quadrupoles (Arc suppressor).

3. INCREASING THE TRANSITION ENERGY BY SUPERPERIODIC MODULATION

To increase the transition energy of the NICA accelerator ring, the possibility of changing the dispersion function by modulating the gradients of the quadrupoles on the rotating arcs of the ring is considered. To do this, consider a superperiod consisting of 3 FODO cells, where the central focusing quadrupole differs from the two edge ones by a larger gradient value [2, 3].

An important requirement in the design of a magneto-optical structure is to ensure zero dispersion in straight sections to ensure the movement of particles along the equilibrium orbit in these sections [4]. This requirement is easily implemented in the case of creating regular rotating arcs composed of identical superperiods. In this case, by providing a zero dispersion value $D = 0$ (as well as the derivative of the dispersion $D' = 0$) at the entrance to the arc, due to the regularity, the output of the arc will also have zero values of the dispersion and its derivative, and therefore on the entire straight section. However, the peculiarity of the given structure of the NICA collider, the presence of missing magnets on the two extreme cells does not make it possible to create a completely regular arc of 4 identical superperiods. Thus, it is necessary to ensure the suppression of dispersion at the edges of the arc. Two possible cases of dispersion suppression are considered:

(1) Dispersion suppression with edge superperiods.

To be precise, the dispersion suppression is carried out by using two edge FODO cells located symmetri-

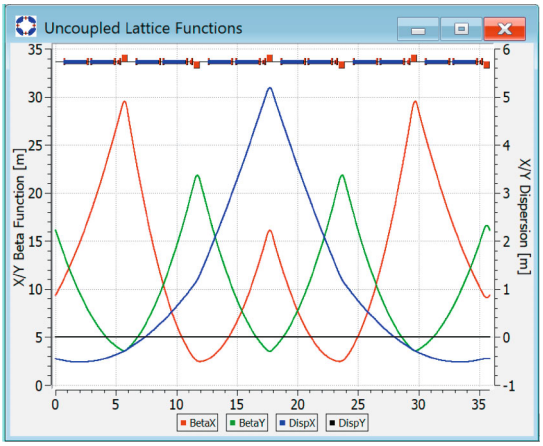

Fig. 4. Modulated superperiod $\nu_S = 0.75$.

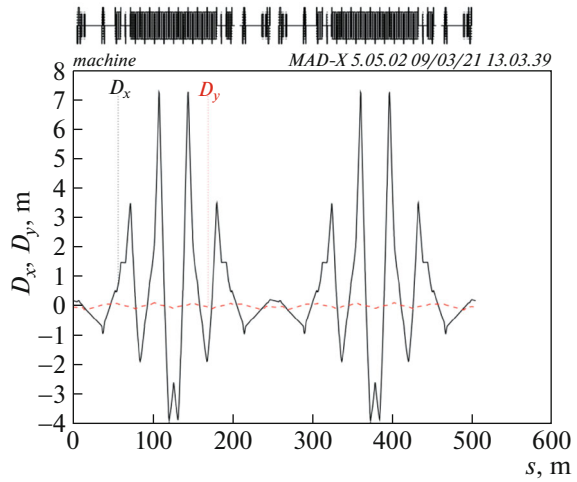

Fig. 5. The dispersion function without the dispersion suppressors on the 2 edge cells.

cally on both sides. Figures 2 and 3 above (ES stands for the edge suppressor) show a schematic diagram of this magneto-optical structure. As can be seen, the two edge FODO cells differ in the presence of a missing-magnet and in these cells, the QFE1 and QFE2 quadrupoles also have different gradients from the main arc quadrupoles and are selected to suppress the dispersion.

(2) Dispersion Suppression by the arc, by selecting the gradients of the quadrupoles of the two families.

Figures 2 and 3 below (AS stands for the arc suppressor) shows a schematic diagram of this magneto-optical structure. This case differs from the first, all the quadrupoles of the arc belong to the first or second family, and the suppression of dispersion is also provided by only 2 families.

The defocusing quadrupoles in both the first and second cases belong to only one QD family.

3.1. Dispersion Suppression by the EDGE Cells of the ARC

3.1.1. Quadrupole Gradients. The choice of the value of the gradients of the arc quadrupoles is determined by two factors:

(1) Obtaining the required value of the transition energy on the entire ring of the collider, which corresponds to $\gamma_{tr} \sim 15–16$;

(2) Provide the number of betatron oscillations on the arc $\nu_{arc} = 3$ in both planes, thereby satisfying the resonant condition for the number of superperiods $S = 4$.

Based on these conditions, we modulate the superperiod with a phase shift on the superperiod $\nu_S = 0.75$ in both planes (Fig. 4).

The collider also consists of 2 arcs and 2 straight sections connecting both arcs. In the middle of the straight sections there are collision points, where it is necessary to provide a small value of the beta function to achieve the required luminosity. The edge superperiod has a missing magnet in 2 cells, thus making the collider arcs not regular and there is a need to suppress the dispersion in straight sections using the introduction of 2 additional families of QFE1 and QFE2 quadrupoles on the edge of the arc, the beta-function and dispersion function of all entire ring are shown on Figure 5.

Figure 6 shows the Twiss parameters of the entire collider ring without introducing the edge quadrupoles QFE1 and QFE2, it is clearly seen that the dispersion is not suppressed in the straight sections.

Table 1 contains the values of quadrupole gradients.

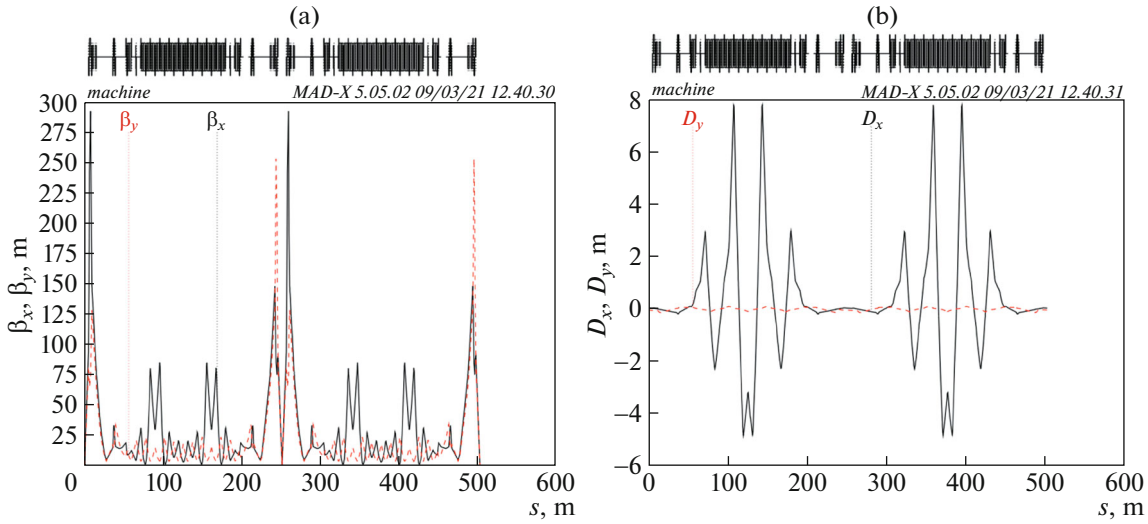

Fig. 6. Dispersion suppression by edge cells of the arc: (a) beta functions; (b) dispersion functions.

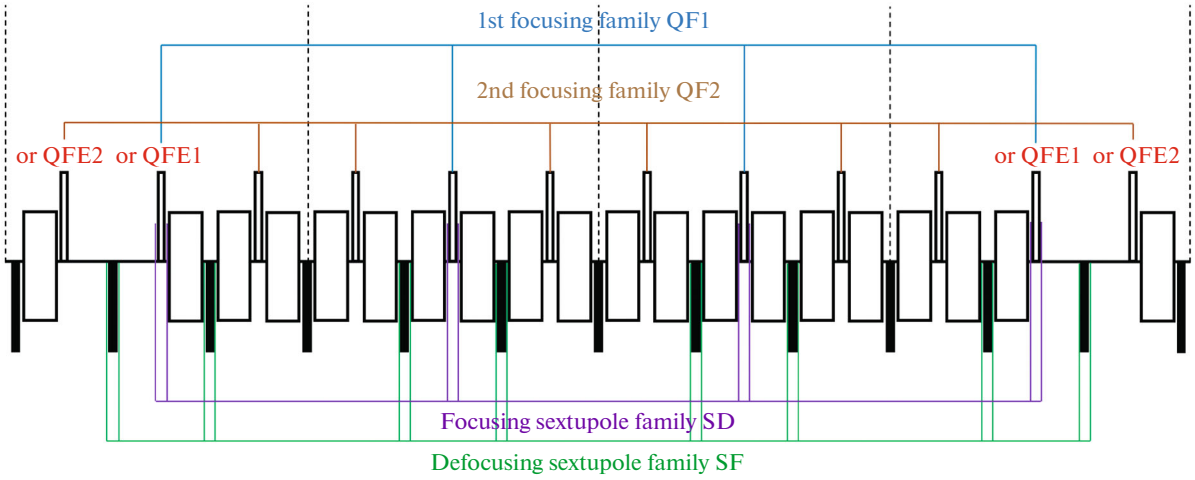

Fig. 7. Schematic diagram of the arrangement of sextupoles in the case of dispersion suppression by the edge superperiods.

As a result, the gamma-transition value is chosen in such a way that $\gamma_{tr} = 15.6$, and tune shift over the circle: $\nu_{x\,\mathrm{arc}} = 3.01$, $\nu_{y\,\mathrm{arc}} = 3.01$.

3.1.2. Sextupoles. The arrangement of the sextupoles also requires that several parameters are taken into account:

(1) First, it is necessary to suppress chromaticity on the entire collider ring [5];

(2) Secondly, to achieve a large value of the dynamic aperture [6], it is necessary to achieve mutual compensation of the sextupoles and make a second order achromat.

To accomplish the first condition, it is necessary to suppress the natural chromaticity, caused by linear elements: quadrupoles and dipoles. To do this, you need to set the sextupoles in the region of non-zero dispersion, on the arcs near the quadrupoles.

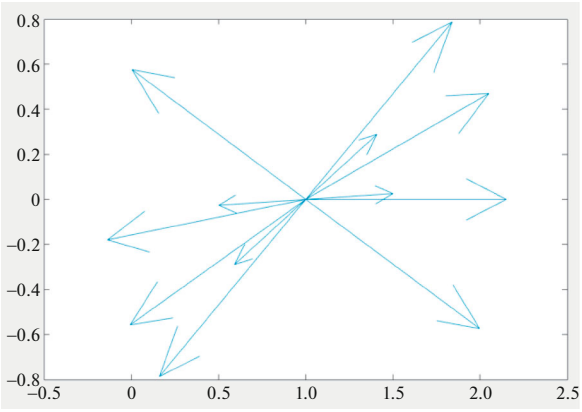

Fig. 8. Vectors of sextuple gradients rotated relative to each other taking into account the phase.

Since the tune shift is on the arc $\nu_{x\,\mathrm{arc}} = 3.01$, $\nu_{y\,\mathrm{arc}} = 3.01$. Thus, at each superperiod, a tune shift occurs 0.75π, including the edge ones. In the described case there is peaks of β-function on arc at quadrupoles QF2. Thus, the phase difference between the QF2 quadrupoles of the first and third (second and fourth superperiod) is not a multiple of $\pi/2$. Simultaneously, the number of betatron oscillations between the central quadrupoles (QF1 or QFE1) of 1 and 3 or 2 and 4 superperiods $\nu_{1-3} = \nu_{2-4} = 1.5$. Thus, by placing the sextupoles of the same family next to the central quadrupoles, it will be possible to ensure mutual suppression of the sextupoles. Figure 7 shows a schematic diagram of the arrangement of sextupoles.

In this case, you need to make sure that the sextupoles are compensated with each other. In Fig. 8, the corresponding gradients are represented as vectors, meanwhile, the rotation of the vector reflects the phase transition between the corresponding sextupoles and is equal to the number of betatron oscillations multiplied by 2π (the first sextuple of the arc was taken as a reference point) [7]. It can be seen that for each vector there is a vector that is directed in the opposite direction and compensates for it.

3.1.3. Dynamic aperture and operating point. Working point for the entire ring 9.44 × 9.44, the same as for the regular structure [8]. Figure 9 shows the dynamic apertures for this working point in both planes for different dp/p. Dynamic aperture in x-plane: 300 mm × mrad; в y-plane: 100 mm × mrad;

3.2. Dispersion Suppression by Two Families of Quadrupoles on the ARC

3.2.1. Quadrupole gradients. This method shows that it is possible to suppress the dispersion in straight

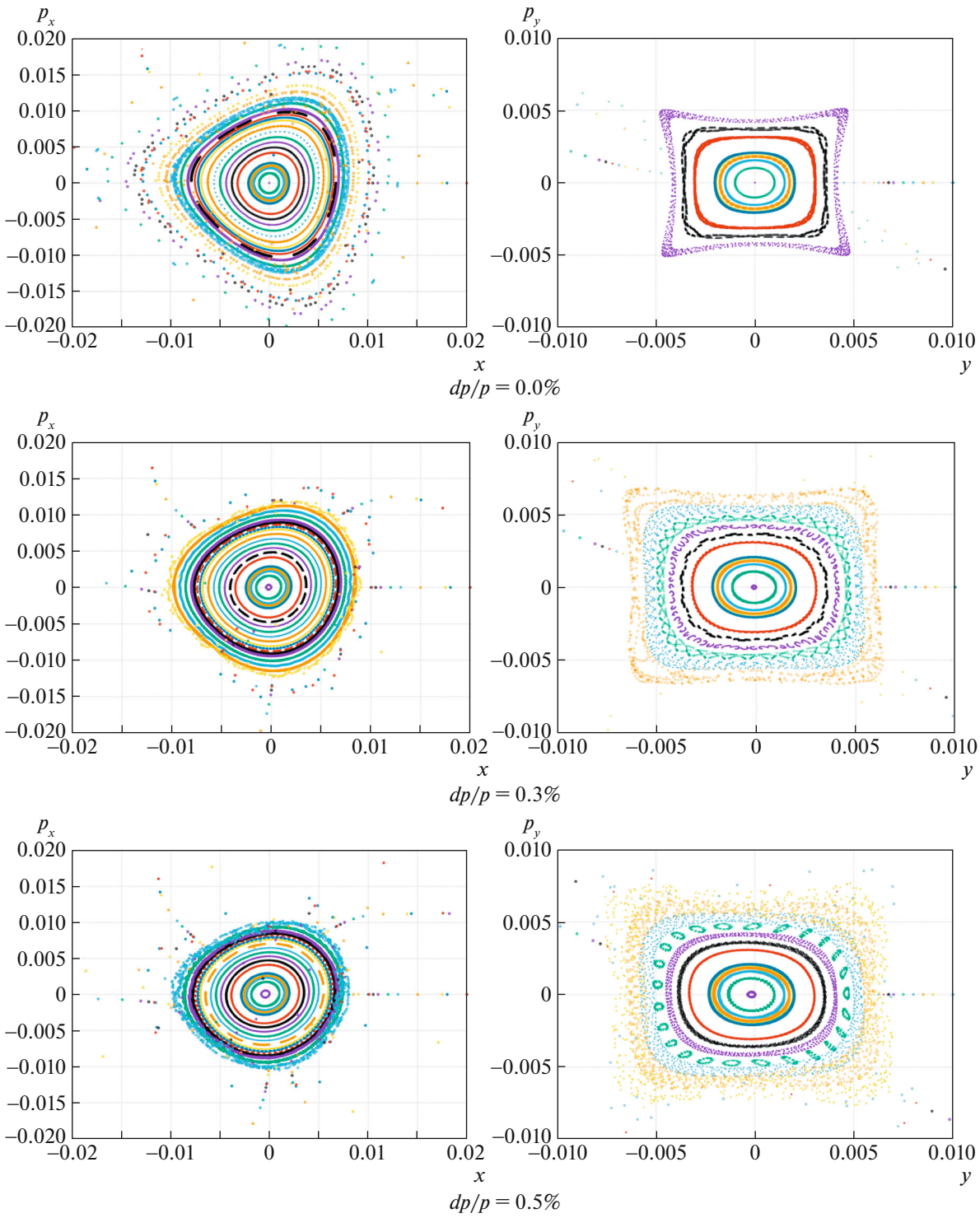

Fig. 9. Dynamic aperture for the case dispersion suppression by edge quadrupoles: x-plane (left); y-plane (right).

sections using only two families of focusing quadrupoles.

It is important to consider here, as in the first case, to perform:

(1) Obtaining the required transition energy value for the entire collider ring, which corresponds to $\gamma_{tr} \sim 15–16$;

(2) Only by using quadrupoles of two families to suppress the dispersion in straight sections.

Initially, the superperiod is selected, as in the first case with a tune shift on the superperiod $\nu_s = 0.75$. Thus, we get the values of the quadrupoles QF1 and QF2 for the entire arc, including at the edges. Table 2 represents values of quadrupole gradients.

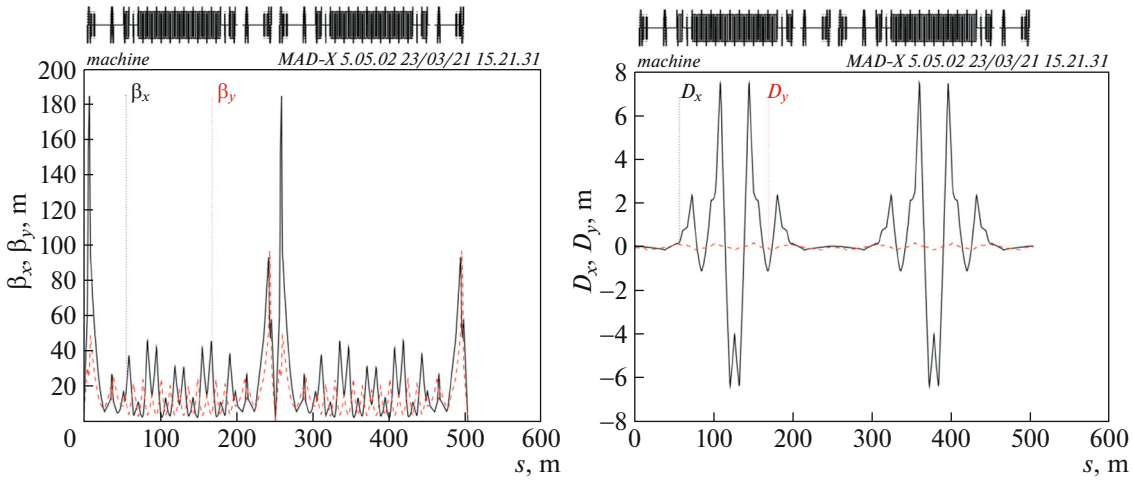

Fig. 10. Dispersion suppression by two families of quadrupoles: beta-functions (left); dispersion functions (right).

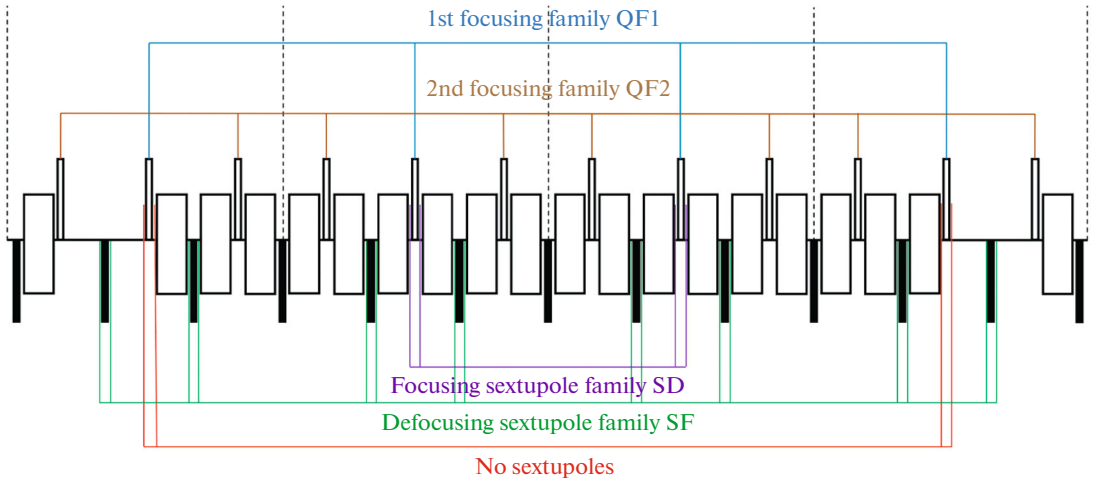

Fig. 11. Schematic diagram of the arrangement of sextupoles in the case of dispersion suppression by two families of quadrupoles.

However, it turns out that the dispersion in the straight sections is not suppressed. For suppression, the values of the quadrupole gradients change, but in this case the phase shift on the arc becomes equal to $\nu_{x\,\mathrm{arc}} = 2.72178$, $\nu_{y\,\mathrm{arc}} = 2.99884$, thus in the x-plane, it is not a multiple of 2π. Beta-functions and dispersion functions are shown in Fig. 10.

In this case, to achieve the required transition energy value, it is necessary to provide a greater modulation of the quadrupole gradients than in the case of dispersion suppression by edge superperiods.

Table 2. Values of arc quadrupole gradients in case of dispersion suppression by two families

Quadrupoles	Gradient, T/m
QF1	28.95
QF2	19.91
QD	–22.6

3.2.2. Sextupoles. Due to the fact, that tune shift on arc is not a multiple of 2π, and also between the central quadrupoles is not a multiple $\pi/2$, and is equal to 1.41, it turns out that the sextupoles do not compensate each other exactly. The arrangement of sextupoles for this case is different from the arrangement of sextupoles in the case of dispersion suppressors at the edges of the arc and is shown in Fig. 11. The SF family is located next to the central quadrupoles of the superperiod QF1, and SD is located next to the defocusing quadrupoles QD, but only those that surround QF1 on the left and right. However, there are no sextupoles of the focusing family in the edge superperiods. This is done to reduce the influence of sextupoles on the dynamic aperture. The suppression of chromaticity is also possible without them, since the main contribution is made by sextupoles 2 and 3 of the superperiod.

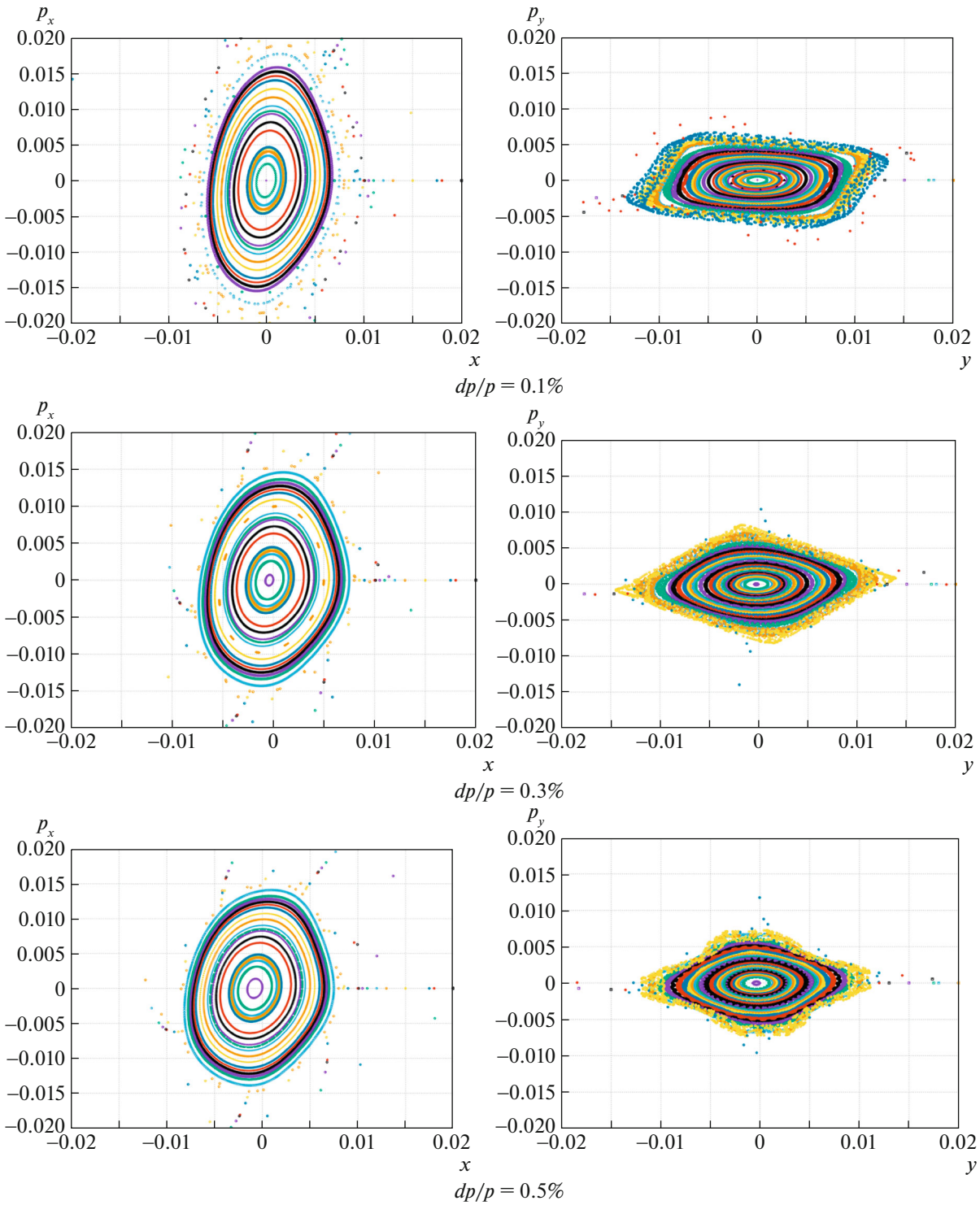

Fig. 12. Dynamic aperture in the case of dispersion suppression by two families of quadrupoles: the x-plane (left); y-plane (right).

3.2.3. Dynamic aperture and operating point. The working point for the entire ring is 9.44 × 9.44, the same as for the regular structure. Figure 12 shows the dynamic aperture for this working point in both planes for different dp/p. Dynamic aperture in x-plane: 300 mm × mrad; in y-plane: 200 mm × mrad.

CONCLUSION

In this paper, we consider one of the possible ways of passing the transition energy in the NICA accelerator complex by increasing the transition energy using superperiodic modulation of quadrupole gradients. Two variants of dispersion suppression are indicated: 1) suppression with two edge cells of arc; 2) suppression with only two arc quadrupole families. For both cases the Twiss parameters are calculated, and methods for arranging the sextupoles necessary to suppress natural chromaticity and mutual compensation of nonlinear effects are proposed. For this cases dynamic apertures are calculated for different dp/p.

REFERENCES

1. Yu. V. Senichev and A. N. Chechenin, J. Exp. Theor. Phys. **105**, 988 (2007).
2. Yu. V. Senichev and A. N. Chechenin, J. Exp. Theor. Phys. **105**, 1141 (2007).
3. Yu. Senichev, A. Chechenin, and S. Kostromin, Vestn. SPb. Univ., Ser. 10: Prikl. Mat. Inform. Prots. Upravl., No. 1, 37 (2011).
4. B. Autin, IEEE Trans. Nucl. Sci. **26** (3) (1979).
5. B. J. Holzer, CERN Yellow Report CERN-2013-001, p. 171.
6. B. Lorentz, A. Lehrach, R. Maier, D. Prasuhn, and H. Stockhorst, and R. Tölle, in *Proceedings of EPAC08, Genoa, Italy*.
7. P. J. Bryant, in *Proceedings of the 5th Course of the CERN Accelerator School, Rhodos, Greece, Sept. 20–Oct. 1, 1993,* Vols. 1, 2.
8. E. M. Syresin, A. V. Butenko, P. R. Zenkevich, S. D. Kolokolchikov, S. A. Kostromin, I. N. Meshkov, N. V. Mityanina, Y. V. Senichev, A. O. Sidorin, and G. V. Trubnikov, Phys. Part. Nucl. **52** (5), 997 (2021). https://doi.org/10.1134/S1063779621050051